HIGHLIGHTS AND BREAKTHROUGHS

Electron channeling to achieve the full potential of mineralogy

NOBUYOSHI MIYAJIMA[1,*]

[1]Bayerisches Geoinstitut, Universität Bayreuth, D-95440 Bayreuth, Germany

[*] E-mail: Nobuyoshi.Miyajima@uni-bayreuth.de

Electron channeling phenomena in electron microscopes are under the spotlight. The determination of site occupancies of select atoms in mineral structures is one of the most intriguing targets in mineralogy. The current extension of electron channeling spectroscopies using a transmission electron microscope (TEM) can provide the site occupancies of particular elements from a sub-micron area (Muto and Ohtsuka, 2017). High angular resolution electron channeling X-ray spectroscopy (HARECXS) sheds light on the understanding of order-disorder transitions and kinematically controlled chemical reactions on the reaction front of the mineral formation process. In addition to spectroscopy, imaging can also be carried out using electron channeling phenomena. The electron channeling contrast from differently oriented grains of the same chemical composition is well known in backscattered electron (BSE) and forward scattered electron (FSE) images in conventional SEM imaging techniques (Reimer, 1998). A rapid change in BSE intensity that occurs as the beam is scanned through the Bragg angle results from significant changes in the Bloch wave excitations (Joy et al., 1982; Kaboli et al., 2015). Electron channeling contrast imaging (ECCI) in a conventional field-emission scanning electron microscope (FE-SEM) has been applied to mineralogy as an alternative imaging tool for observing individual dislocations in rock-forming minerals (Miyajima et al., 2017). Analysis of forsterite deformation mechanisms has also been carried out with ECCI and electron backscatter diffraction (EBSD) (Kaboli et al., 2017; Kaboli et al., 2016). In the current issue of *American Mineralogist*, Igami et al. (2018) present a HARECXS study on Al/Si order-disorder in sillimanite as one of the most advanced applications of electron channeling spectroscopy.

What is electron channeling? Electron channeling is the anomalous interaction of incident electrons with a single crystal that is oriented under both a Bragg condition and zone axis condition. In the former setting, the electron beam is pseudo-parallel to the (hkl) crystallographic plane, which is called the "two-beam condition with ***g*** = hkl" in the TEM community. In the latter scenario, the beam is along the <uvw> direction. Close to the Bragg orientation or along the zone axis, standing waves (Bloch waves) generated by the incident beam strongly interact with the crystallographic planes or atomic columns. Thus, electrons flow strongly along characteristic crystallographic planes, i.e., current densities related to electron inelastic interactions such as X-ray spectroscopy, electron-energy loss-spectroscopy (EELS), and BSE are strongly localized at the planes (planar channeling) or along the zone axis (axial channeling). Using the channeling effects in energy-dispersive X-ray spectroscopy (EDXS), the site and its occupancy by a particular element in the target crystal can be determined from the variations of X-ray intensity with changing crystal orientation, which is called "ALCHEMI (Atom Location by Channeling–Enhanced Microanalysis)" (Tafto, 1982). The maximum channeling effect, i.e., maximum current density along a crystallographic plane (or atomic column) or the other plane (column), is controlled by a small deviation (s) of positive and negative value ($s < 0$ and $s > 0$, respectively) against the Bragg condition ($s = 0$).

To obtain planar channeling in TEM, precise crystal orientation alignment across a Bragg angle is necessary. Figure 1 shows three electron diffraction conditions for planar channeling. Figure 1a shows an Ewald sphere and diffraction conditions with small deviations, s

< 0 and $s > 0$, which are an excitation error from a specific Bragg angle. The equation, $\boldsymbol{K}' - \boldsymbol{K} = \boldsymbol{g} + \boldsymbol{s}$, where K' and K are the wave vectors of the diffracted and incident beams, respectively, g is the reciprocal-lattice vector of the crystal, and s is the excitation error, indicates the diffraction condition under which a diffraction intensity in electron diffraction can be obtained. Figure 1b illustrates the relationship between diffraction conditions and corresponding electron diffraction patterns. For planar ALCHEMI analysis, at least these two channeling conditions must be chosen with positive and negative s in the diffraction condition. When these conditions are maintained for EDXS and EELS measurements, a strong anomaly in those spectra is detected due to a modulation of the current density in the crystal.

Figure 2 is a schematic example of the three channeling conditions (Spence and Tafto, 1983; Tafto and Spence, 1982). Firstly, a specific crystal direction must be found in which two different cation sites (in this case, A and B sites) lie in separated arrays. In these three different crystal orientations, the density of incident electrons strongly localizes depending on the standing wave of electrons, as well as selective excitation due to inelastic process (EDXS and EELS). In this example, Al is located on the B-site with Si. If the B-site is selectively excited, the intensity of the Si-K and Al-K line peaks increase. From this correlation, we can determine the site preference of an impurity in an orthorhombic perovskite (Miyajima et al., 2004).

How is the site localization of inelastic events used to determine site occupancies? The correlation between current density and site occupancy, which results in anomalous intensity ratios in channeling spectroscopy, is based on the assumption that the ionization of target elements is well localized on specific atomic sites during inelastic scattering events. In reality, localization variations (i.e., delocalization) are inversely related to both the mean inelastic scattering angle associated with the ionization event and to the emitted X-ray and electron loss energies (Spence et al., 1988). This is called the "delocalization problem."

How to overcome the "delocalization problem"? One of the best tactics is a statistical ALCHEMI approach (Turner et al., 1991). This method involves standard multivariate analysis to obtain the best fit and uncertainties of the impurity counts as a linear combination of counts from the host species. The ALCHEMI method provides fractional partitioning values and concentrations of an impurity species between host sites, together with standard estimates of reliability.

How to further improve? In the recently developed HARECXS method, variations of experimental EDX spectra intensity against incident beam directions are compared with theoretical profiles of a known structure generated from a fast electron dynamical simulation. In practice, tediously fine alignment of the crystal orientation is not required to maintain channeling conditions, such as $s < 0$ and $s > 0$, against the Bragg condition in the case of planar ALCHEMI. A set of EDX spectra is automatically obtained as a function of beam-tilt direction by rocking the incident electron beam with a fixed pivot point on the sample surface. A new statistical approach to determine site occupancies by multivariate analysis of the least squares fitting of a linear combination of completely ordered and completely disordered structures was developed on the basis of simulated HARECXS profiles calculated by the program ICSC (Oxley and Allen, 2003). The profile simulation is based on the ionized cross sections in EDXS. Statistical comparison with a simulated profile can improve the accuracy of the site occupancy determination (Muto and Ohtsuka, 2017).

Igami et al. (2018) applied the HARECXS method to determine the Al/Si order parameter in sillimanite at high temperature. Although the sillimanite coexisted with mullite at the submicrometer scale, the analytical TEM method demonstrates a potential nanoprobe to measure site-occupancies of relatively light and neighboring elements in chemically complex minerals. The HARECXS method is useful for the determination of site occupancies of rock-forming minerals involving order-disorder in solid solutions, such as Mg/Fe in olivine (Tafto and Spence, 1982) and pyroxene and Al/Si in feldspar (Mclaren and Fitz Gerald, 1987). The method provides new information about the formation process of minerals with complicated microtextures that can only be resolved by TEM. A combination of HARECXS with EELS in TEM has already been applied to quantitative analysis of the atomic configuration and valence states in lithium manganese spinel (Yamamoto et al., 2016). The simultaneous data acquisition and analysis with dynamical electron diffraction theories provide a simple, practical, and automated measurement methodology to obtain quantitative information specific to both the element and site at the submicron scale.

In addition, a combination of the electron channeling pattern (ECP) in FE-SEM with ultra-high probe currents of 10 to several 100 nanoamperes (nA) is interesting for channeling EDXS equipped with a large solid angle silicon drift detector (Fig. 3). The incident electron beam, from the crossover point of the final lens, scans over a large sample area at low magnification, resulting in a larger angle against the surface of the bulk sample in the ECP. The ray path is in the principle of reciprocity with that of a rocking incident beam with a fixed pivot point on the sample surface in HARECXS (Fig. 1 in Igami et al., 2017). Kikuchi bands in the ECP of single-crystal minerals should be associated with enhanced X-ray emission, which is an analogue of extinction contours in a thin Au foil (Duncumb, 1962). Selected Kikuchi bands in a mineral structure should show channeling correlations between the current density and site occupancy of elements in SEM-EDXS. Further development of this SEM-EDXS technique may make possible the characterization of bulk samples without the tedium of TEM sample preparation.

Finally, the current extension of electron channeling into spectroscopy and imaging can provide the site occupancies of particular elements from a sub-micron area of rock-forming minerals by TEM. Electron channeling can facilitate high quality scanning “diffraction contrast” imaging of crystal defects in bulk samples by FE-SEM. Orientation-dependent techniques in analytical electron microscopy combined with dynamical electron diffraction provide intriguing new information in mineralogy.

REFERENCES CITED

Duncumb, P. (1962) Enhanced X-ray emission from extinction contours in a single-crystal gold film. The Philosophical Magazine: A Journal of Theoretical Experimental and Applied Physics, 7(84), 2101-2105.

Igami, Y., Kuribayashi, T., and Miyake, A. (2018) Quantitative determination of Al/Si order in sillimanite by high angular resolution electron channeling X-ray spectroscopy. American Mineralogist, in press.

Igami, Y., Ohi, S., and Miyake, A. (2017) Sillimanite-mullite transformation observed in synchrotron X-ray diffraction experiments. Journal of the American Ceramic Society, 100(10), 4928-4937.

Joy, D.C., Newbury, D.E., and Davidson, D.L. (1982) Electron Channeling Patterns in the Scanning Electron-Microscope. Journal of Applied Physics, 53(8), R81-R122.

Kaboli, S., Burnley, P.C., Xia, G., and Green, H.W. (2017) Pressure Dependence of Creep in Forsterite Olivine: Comparison of Measurements From the D-DIA and Griggs Apparatus. Geophysical Research Letters, 44(21), 10939-10947.

Kaboli, S., Demers, H., Brodusch, N., and Gauvin, R. (2015) Rotation contour contrast reconstruction using electron backscatter diffraction in a scanning electron microscope. Journal of Applied Crystallography, 48, 776-785.

Kaboli, S., Gauvin, R., and Burnley, P. (2016) Deformation Analysis of Forsterite Olivine Using Electron Channeling Contrast Imaging and Electron Backscatter Diffraction. Microscopy and Microanalysis, 22(S3), 1792-1793.

Mclaren, A.C., and Fitz Gerald, J.D. (1987) Cbed and Alchemi Investigation of Local Symmetry and Al, Si Ordering K-Feldspars. Physics and Chemistry of Minerals, 14(3), 281-292.

Miyajima, N., Langenhorst, F., Frost, D.J., and Yagi, T. (2004) Electron channelling spectroscopy of iron in majoritic garnet and silicate perovskite using a transmission electron microscope. Physics of the Earth and Planetary Interiors, 143, 601-609.

Miyajima, N., Li, Y., Abeykoon, S., and Heidelbach, F. (2017) Electron channelling contrast imaging of individual dislocations in geological materials using a field emission scanning electron microscope equipped with an EBSD system. European Journal of Mineralogy, 30(1).

Muto, S., and Ohtsuka, M. (2017) High-precision quantitative atomic-site-analysis of functional dopants in crystalline materials by electron-channelling-enhanced microanalysis. Progress in Crystal Growth and Characterization of Materials, 63(2), 40-61.

Oxley, M.P., and Allen, L.J. (2003) ICSC: a program for calculating inelastic scattering cross sections for fast electrons incident on crystals. Journal of Applied Crystallography, 36(3 Part 2), 940-943.

Reimer, L. (1998) Scanning Electron Microscopy. Physics of Image Formation and Microanalysis. . 528 p.

Spence, J.C.H., Kuwabara, M., and Kim, Y. (1988) Localization Effects on Quantification in Axial and Planar Alchemi. Ultramicroscopy, 26(1-2), 103-112.

Spence, J.C.H., and Tafto, J. (1983) Alchemi - a New Technique for Locating Atoms in Small Crystals. Journal of Microscopy-Oxford, 130(May), 147-154.

Tafto, J. (1982) The Cation-Atom Distribution in a $(Cr,Fe,Al,Mg)_3O_4$ Spinel as Revealed from the Channeling Effect in Electron-Induced X-Ray-Emission. Journal of Applied Crystallography, 15(Aug), 378-381.

Tafto, J., and Spence, J.C.H. (1982) Crystal Site Location of Iron and Trace-Elements in a Magnesium-Iron Olivine by a New Crystallographic Technique. Science, 218(4567), 49-51.

Turner, P.S., White, T.J., Oconnor, A.J., and Rossouw, C.J. (1991) Advances in Alchemi Analysis. Journal of Microscopy-Oxford, 162, 369-378.

Yamamoto, Y., Kataoka, K., Akimoto, J., Tatsumi, K., Kousaka, T., Ohnishi, J., Takahashi, T., and Muto, S. (2016) Quantitative analysis of cation mixing and local valence states in $LiNixMn_{2-x}O_4$ using concurrent HARECXS and HARECES measurements. Microscopy, 65(3), 253-262.

Figure captions

Figure 1. (a) Schematic illustration of channeling conditions with excitation error deviations $s < 0$, $s = 0$ (Bragg condition), and $s > 0$ in transmission electron microscopy. Electron diffraction spots can be detected when the equation $\boldsymbol{K'} - \boldsymbol{K} = \boldsymbol{g} + \boldsymbol{s}$ is satisfied. (b) Identification of the deviation parameter s from a geometrical relation between diffraction spots and Kikuchi lines in a systematic diffraction condition along the $\boldsymbol{a^*}$-reciprocal direction, normal to the {h00} plane, in a cubic spinel structure. The exciting cation sites (tetrahedral or octahedral) in the spinel structure depend on the conditions with $s < 0$ and $s > 0$, respectively.

Figure 2. Illustration of the three conditions in planar channeling EDXS of an ABO_3-perovskite structure with $Mg(Si,Al)O_3$ composition, e.g., bridgmanite. The *Diffraction I* and *III* conditions are excited for the A-site and B-site with higher current densities, respectively, while *Diffraction II* is a non-channeling condition with a homogeneous current density. The corresponding EDXS spectra are displayed in the lowest line, indicating variations of intensity ratios with changing conditions.

Figure 3. (a) Electron channeling pattern of a single crystal olivine in a backscattered electron (BSE) image at low magnification under backscattered geometry. A Kikuchi band runs from the lower left to upper right showing a discontinuity over a subgrain boundary (indicated by an asterisk), which is visible in forward scattered electron (FSE) image (b). The left insets are EDXS maps of Mg-K and Si-K lines from the dotted square. The intensity distribution roughly reflects that of the BSE image with a delocalization. (b) Corresponding FSE image under 70-

degree sample tilt conditions. The contrast comes from the Kikuchi band contrast in the electron backscattering diffraction (EBSD) geometry.

Figures

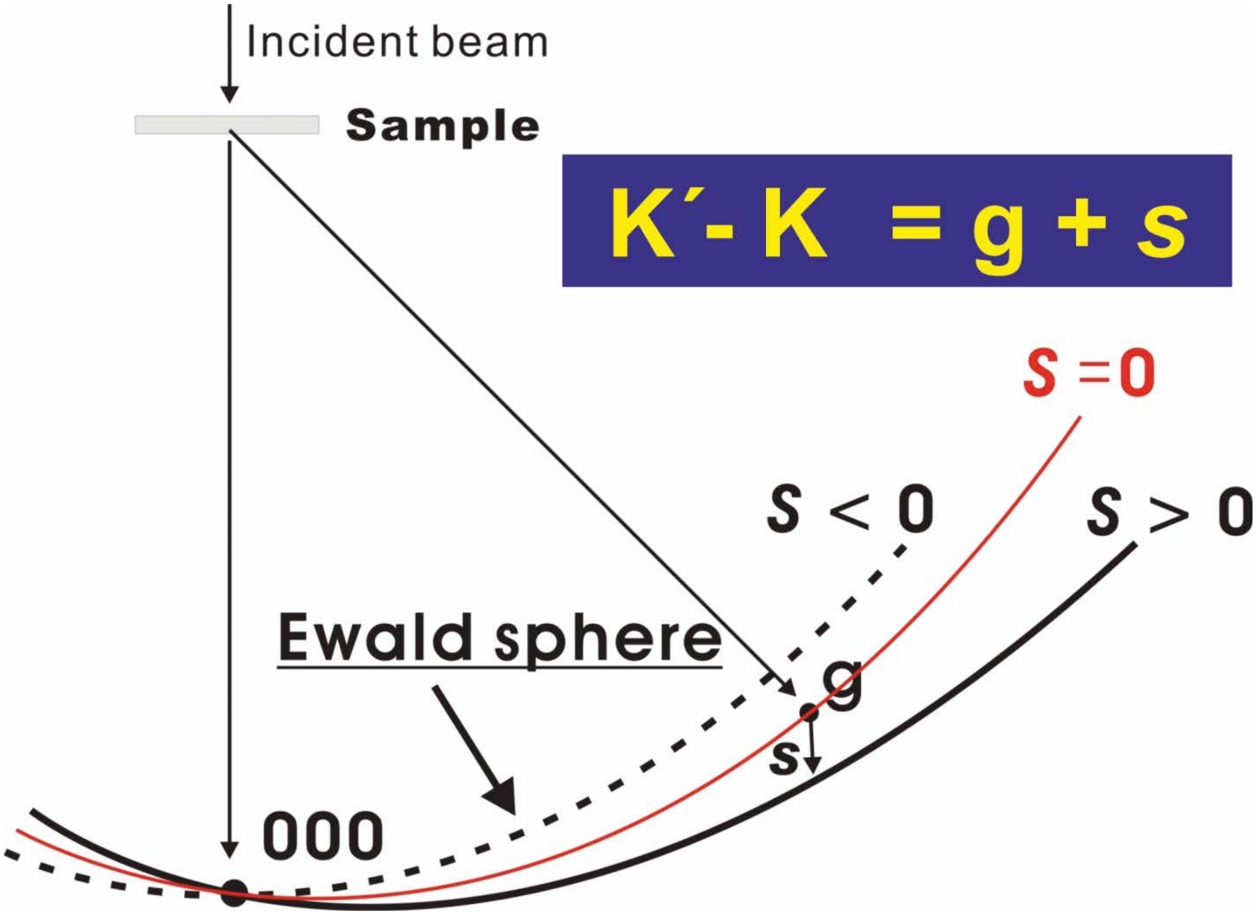

(a)

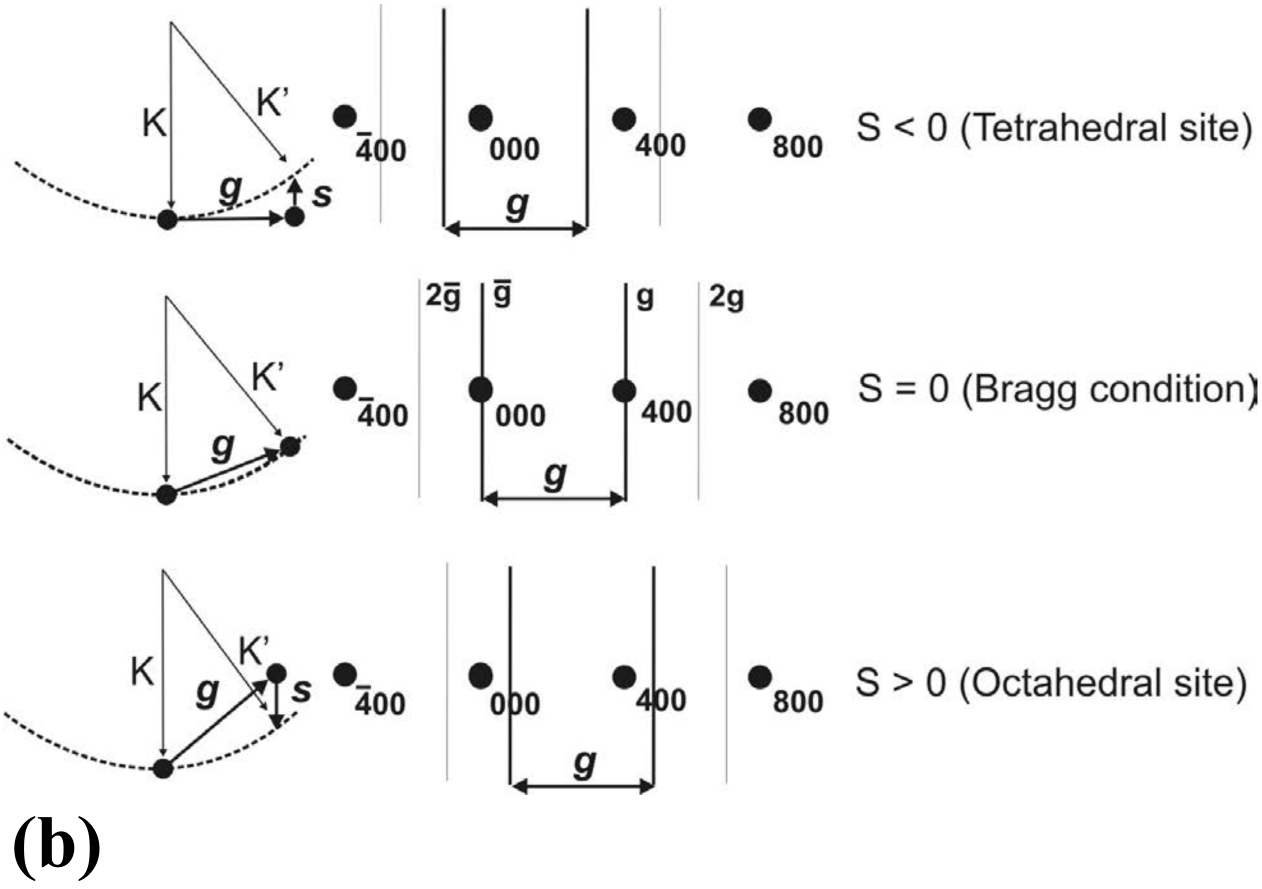
K
K'
g
s
$\bar{4}00$
000
400
800
g
S < 0 (Tetrahedral site)
$2\bar{g}$
$\bar{g}$
g
2g
K
K'
g
$\bar{4}00$
000
400
800
g
S = 0 (Bragg condition)
K
K'
g
s
$\bar{4}00$
000
400
800
g
S > 0 (Octahedral site)
(b)

Figure 1.

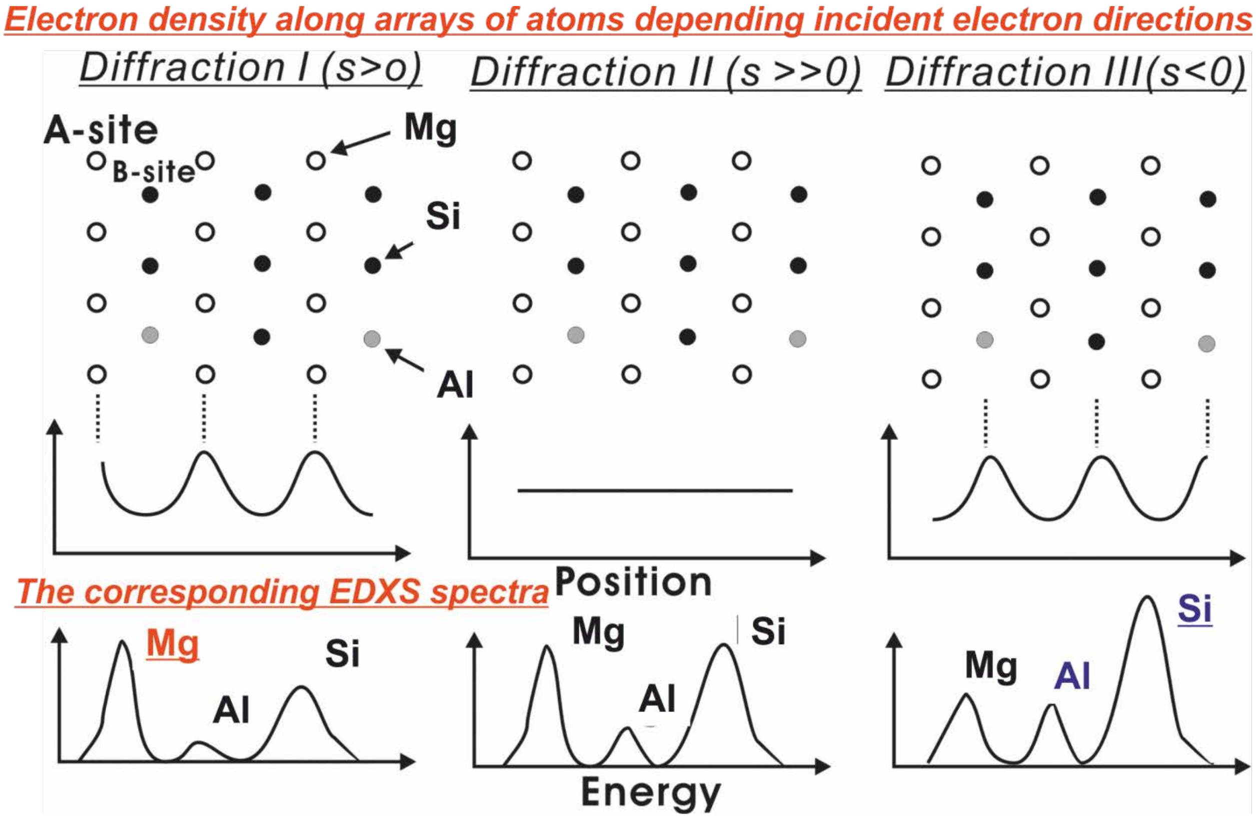
Electron density along arrays of atoms depending incident electron directions
Diffraction I (s>o)
Diffraction II (s >>0)
Diffraction III(s<0)
A-site
B-site
Mg
Si
Al
Position
The corresponding EDXS spectra
Mg
Al
Si
Mg
Al
Si
Mg
Al
Si
Energy

Figure 2.

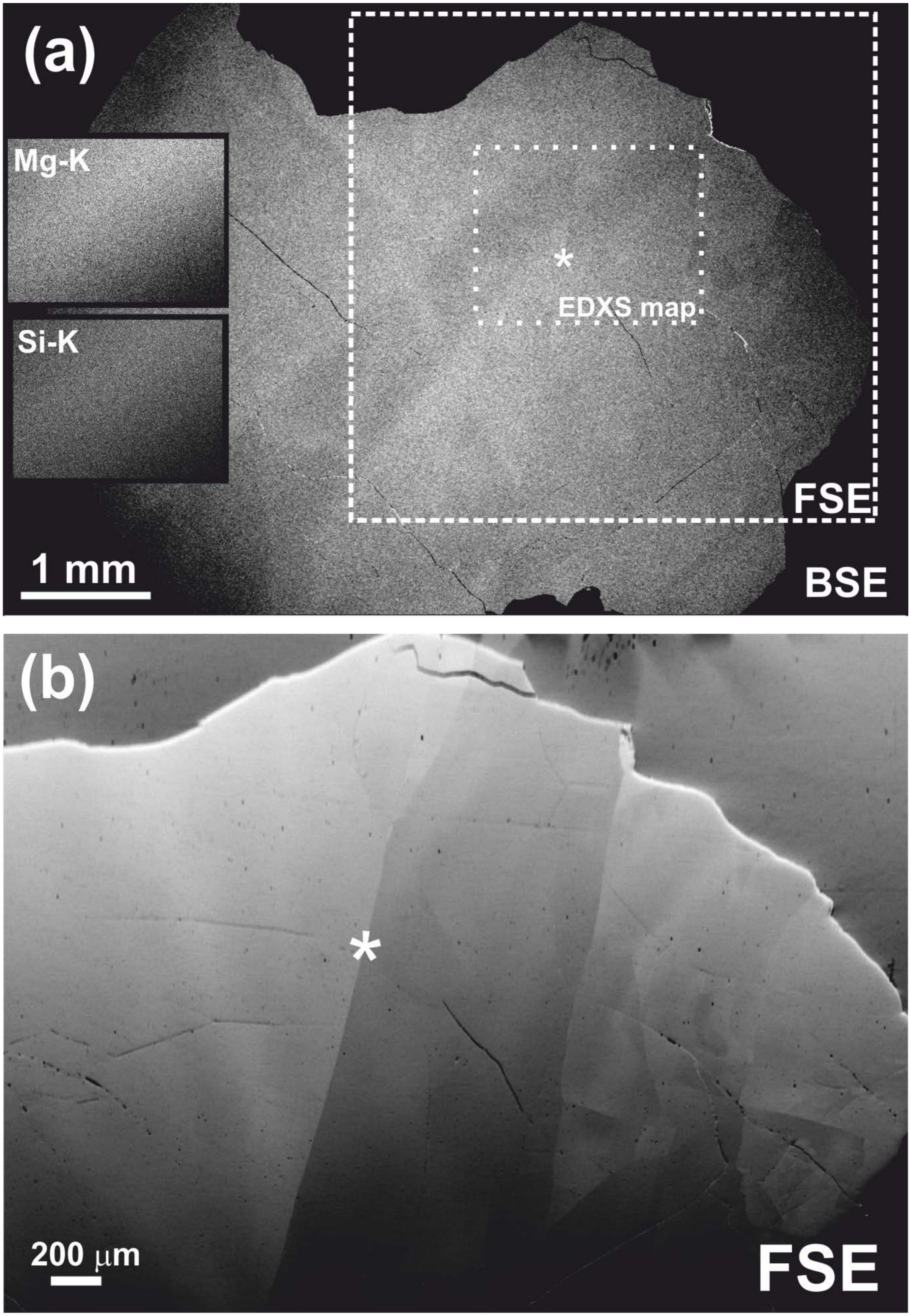
(a)
Mg-K
Si-K
*
EDXS map
FSE
1 mm
BSE
(b)
*
200 μm
FSE

Figure 3.